Modeling the Potential for Fire Ignition and Large Fire Occurrence in Santa Barbara County, California

Heather L. Rustigian-Romsos, John A. Gallo, Wayne D. Spencer, and Alexandra D. Syphard

Conservation Biology Institute

May, 2021

A Component of the Regional Priority Plan Project for Santa Barbara County: Planning, Mapping, and Assessment Phase

Funded by California Department of Conservation, via California Coastal Conservancy, via Cachuma Resource Conservation District

Preferred Citation:

Rustigian-Romsos, H.L., J.A. Gallo, W.D. Spencer, and A.D. Syphard. 2021. Modeling the potential for fire ignition and large fire occurrence in Santa Barbara County, California. Conservation Biology Institute. https://doi.org/10.6084/m9.figshare.14417837

Table of Contents

Executive Summary

We used historical fire occurrence data to evaluate the relative probability of wildfire ignition and occurrence of large fires across Santa Barbara county, California, under both historical and projected future conditions. The resulting probability layers are intended to support a Regional Priority Plan to reduce wildfire risk and improve forest and habitat health.

We statistically compared locations of fire ignitions and large fires ($\geq$ 40-ha) to environmental variables likely to influence where fires start and how they spread (vegetation, terrain, land-use, and climate variables). We used the most predictive variables to create multivariate models of fire ignition risk and the risk of large fire using the MaxEnt program. In addition to estimating risk now using the baseline conditions (1980-2010) we also estimated these risks into the future (2020-2050) using two available general circulation models (GCM) - CNRM-CM5 (“cool/wet” conditions) and MIROC5 (“hot/dry” conditions), and we used the RCP 8.5 “business as usual” emissions scenario for both. To consider fire-climate-vegetation interactions under future climates, simulated vegetation predictors derived from a process-based dynamic vegetation model called MC2 were included. We also mapped the percent change of fire ignition and large fire occurrence risk for any given location from current to future conditions.

We tested the models by seeing how well they predicted some past fire ignitions and large fires that had been randomly set aside from those fires used to train the models. Average test AUC values (a measure of model discrimination) were 0.72 for fire ignition and 0.67 for large fire occurrence, suggesting the models performed satisfactorily with moderate predictive power.

Fire Ignition Risks - Baseline

Distance to development and distance to roads were the most important contributors to ignition risk. Minimum temperature and annual precipitation were of moderate importance. Fire ignition risk varies greatly across Santa Barbara County, but is concentrated on flat slopes and in lower elevation areas, such as Nipomo Valley in the northwest, Santa Ynez Valley in the central part of the county, Cuyama Valley in the north, and Ojai Valley in the southeastern part of the study region. There is also a large zone at higher risk on the coast, in the greater Santa Barbara area.

Fire Ignition Risks - Futures

Under CNRM-CM5 (cool/wet) future projections, fire ignition risk patterns are similar to the baseline, with the following differences. Percent change from baseline was highest in mountainous areas (San Rafael and Santa Ynez), southwest of Lompoc, and in the Nipomo valley. Large decreases in fire ignition risk are projected under CNRM-CM5 in north-central and northeastern portions of the region - Caliente Range, Sierra Madre. Across the entire landscape, there was an average increase in projected fire ignition risk of 7%.

Under MIROC5 (hot/dry) conditions, there was a projected contraction in areas of high fire ignition risk over most of the region, most notably in the greater Santa Barbara region, Santa Maria Valley, and Cuyama Valley. The very limited areas with increased projected fire ignition risk under MIROC5 are concentrated in inland areas at higher elevations around Matilija Wilderness, Pine Mountain, and Topatopa Mountains following patterns in increased summer precipitation and dead wood carbon. Across the entire landscape, there is an average decrease in projected fire ignition risk of 18% across the landscape.

Large Scale Fire occurrence - Baseline

Topographic heterogeneity, higher wind speeds, higher minimum temperature, and higher annual precipitation were the most important contributors to the occurrence of large scale fires. Areas at greater risk for large fires in the region are at predominantly at higher elevations with steep slopes, along the Irish Hills in the west, Santa Ynez-Sulphur Mountains along the coast, Sierra Madre Mountains to the north, San Rafael Range in the central part of the region, and Topatopa Mountains to the east.

Large Scale Fire occurrence - Future

Under both CNRM-CM5 (cool/wet) and MIROC5 (hot/dry) projections, large fire risks are slightly greater than under the baseline, with the following differences. Minimum temperature and dead wood carbon, moderately important predictors in the large fire risk model, show similar patterns of increase relative to baseline under both GCMs. Percent change in projected large fire risk under CNRM-CM5 is highest in the northeastern part of the region around San Emigdio Mesa and San Guillermo Mountain, around the Topatopa Mountains in the east, and also along the Sierra Madre and San Rafael Mountains. Across the entire landscape, there is an average increase in projected large fire risk of 9% under CNRM-CM5. Highest projected increases in large fire risk are in small patches around San Emigdio Mesa and San Guillermo Mountain under MIROC5, with an average increase of 8% across the landscape.

We emphasize that fire risk modeling is inherently uncertain given the stochastic nature of fire and how it is affected by factors not available for statistical analyses, and that therefore these results must be interpreted with caution.

Introduction

Santa Barbara County is ravaged by fires every year, this has only gotten worse as the climate changes. Policy makers and land managers would like to have a better idea on which areas within the county are more vulnerable to fires in the future, to be able to take necessary preventative actions. There are few risk models that are able to guide such planning and none based on local conditions and with high data resolution. Two key indicators of vulnerability to fires are the risk of large fire occurrences and the risk of ignitions. In this project we model these two indicators of vulnerability to fires across the county using the best available data and modelling tools we have.

The objective of this project was to use fire occurrence and perimeter data to evaluate the relative probability of wildfire ignition and occurrence of large fires across Santa Barbara county, California, under historical and projected future conditions. The resulting probability layers are intended to support a Regional Priority Plan to reduce wildfire risk and improve forest and habitat health.

The results should be interpreted with caution. Modeling fire risk is an uncertain task given the stochastic nature of fire and how its effects are influenced by ignition timing and location, terrain, fuel conditions, weather conditions, and firefighter tactics during a fire. Our intent was to map the potential for large fires based on available, landscape-scale, and longer-term data, not to predict real-time fire behavior nor to make precise predictions about future fires.

Methods

We used an approach similar to Syphard et al. (2018) to develop statistical correlative models relating fire occurrence patterns over average conditions in the past and map projected future fire occurrence by combining Maxent ('presence-only' software for modeling distributions; Phillips et al. 2006) with outputs from a dynamic vegetation model and downscaled climate model. MaxEnt compares occurrence points with a sample of background points to create a prediction of relative risk. MaxEnt has been successfully used in a range of wildfire analyses (Bar-Massada et al. 2012, Parisien et al. 2016, Davis et al. 2017, Syphard et al. 2018, Tracy et al. 2018, Syphard et al. 2019).

We statistically compared locations of fire ignitions and large fires (≥ 40-ha) to environmental variables likely to influence where fires start and how they spread (vegetation, terrain, land-use, and climate variables). We used the predictive variables to create separate multivariate models of fire ignition and large fire occurrence (i.e., likelihood or risk of a pixel burning as a fire spreads) risk using the MaxEnt program, training and testing models with fire ignition points and randomly distributed points within large fire perimeters. We considered 18 variables and settled on the most parsimonious set of 11 variables for the fire ignition analysis and 9 variables for the large fire occurrence analysis.

We also wanted to estimate these risks in the future, and identify where the risks increase or decrease. To consider fire-climate-vegetation interactions and feedbacks under future climates, simulated vegetation predictors derived from a process-based dynamic vegetation model (MC2; Bachelet et al. 2015) were used in place of static vegetation maps (Syphard et al. 2018). Our models were calibrated using baseline conditions (1980-2010) and projected to future conditions (2020-2050) under two general circulation models for which both simulated vegetation and downscaled climate data were available. In addition to these 6 model outputs, we averaged the future outputs for each correlative model. Finally, we mapped the percent change of fire ignition and large fire occurrence risk risk for any given location from current to future conditions.

Study Area

Our area of interest includes Santa Barbara County, California as well as portions of adjacent San Luis Obispo, Ventura, and Kern Counties and encompasses most of the Los Padres National Forest (Figure 1).

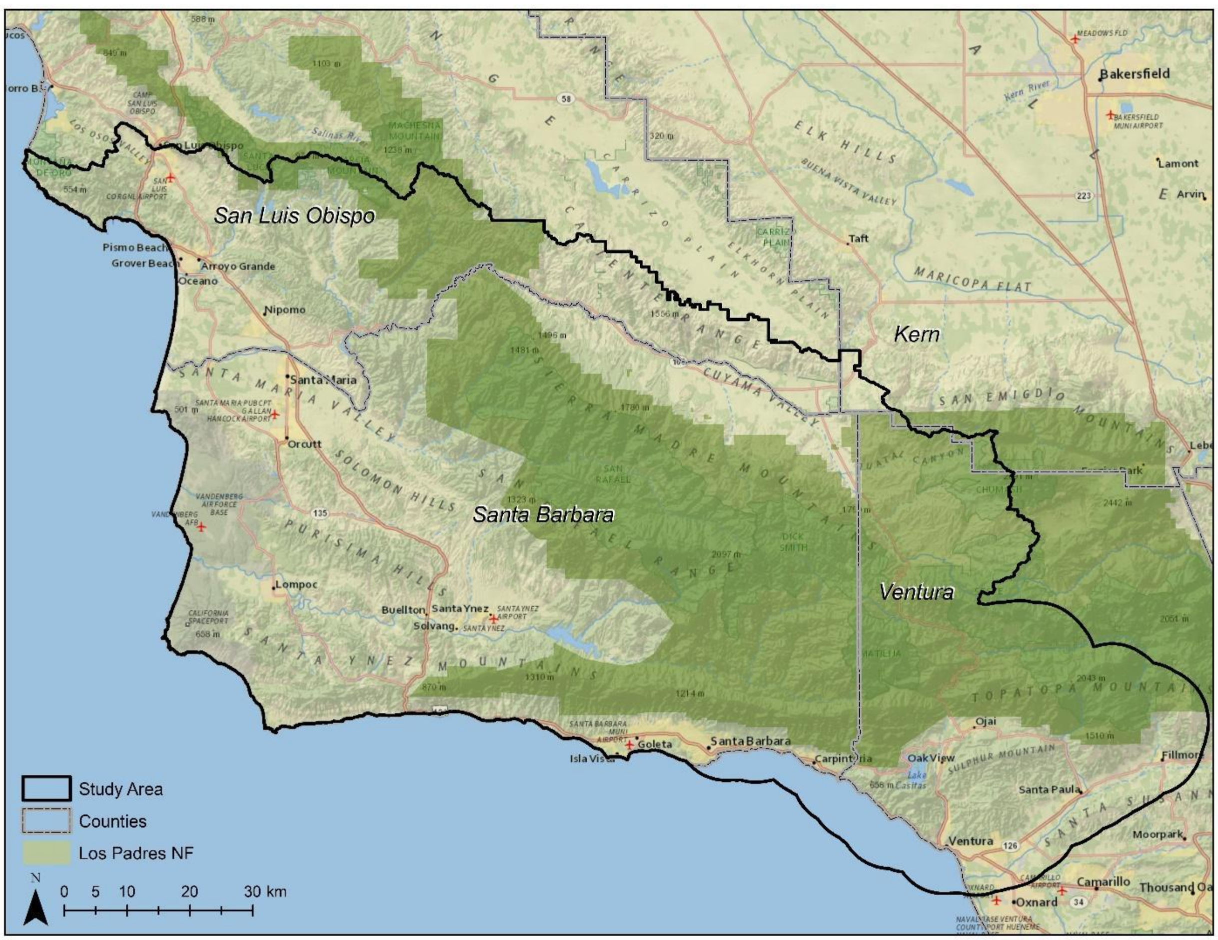

Figure 1. Study area.

Fire Data

We integrated multiple datasets to capture fire activity patterns over the last 40 years, including the 30 years covered by the baseline climate and simulated vegetation data (1980-2010) and extending through 2019 for data on fire occurrence.

For our fire ignition risk model, we used ignition points from the National Interagency Fire Program Analysis Fire-Occurrence Database[1] within the study area, for the period 1992-2015. We augmented this database with other sources covering federal land to capture ignition points from 1980-1991 and 2016-2019: Federal Wildland Fire Occurrence Data[2] were available for 1980-1991 and 2016, while FIRESTAT Fire Occurrence – Yearly Update[3] covered 2017-2019. Ignition points from these 3 datasets within our area of interest totaled 2302 points, which we thinned to 500m minimum nearest neighbor distance (based on testing of best distance in the northern Sierra Nevada - Southern Cascades; Syphard et al. 2018) to increase spatial independence and reduce spatial autocorrelation and model performance inflation (Veloz 2009, Boria et al. 2014). This left 1353 points, which we divided into model training points (80%, n = 1081) and evaluation points (20%, n = 272; Figure 2).

[1] FPA-FOD, https://www.fs.usda.gov/rds/archive/Catalog/RDS-2013-0009.4/
[2] https://data-usfs.hub.arcgis.com/datasets/national-usfs-fire-occurrence-point-feature-layer
[3] https://data.fs.usda.gov/geodata/edw/datasets.php

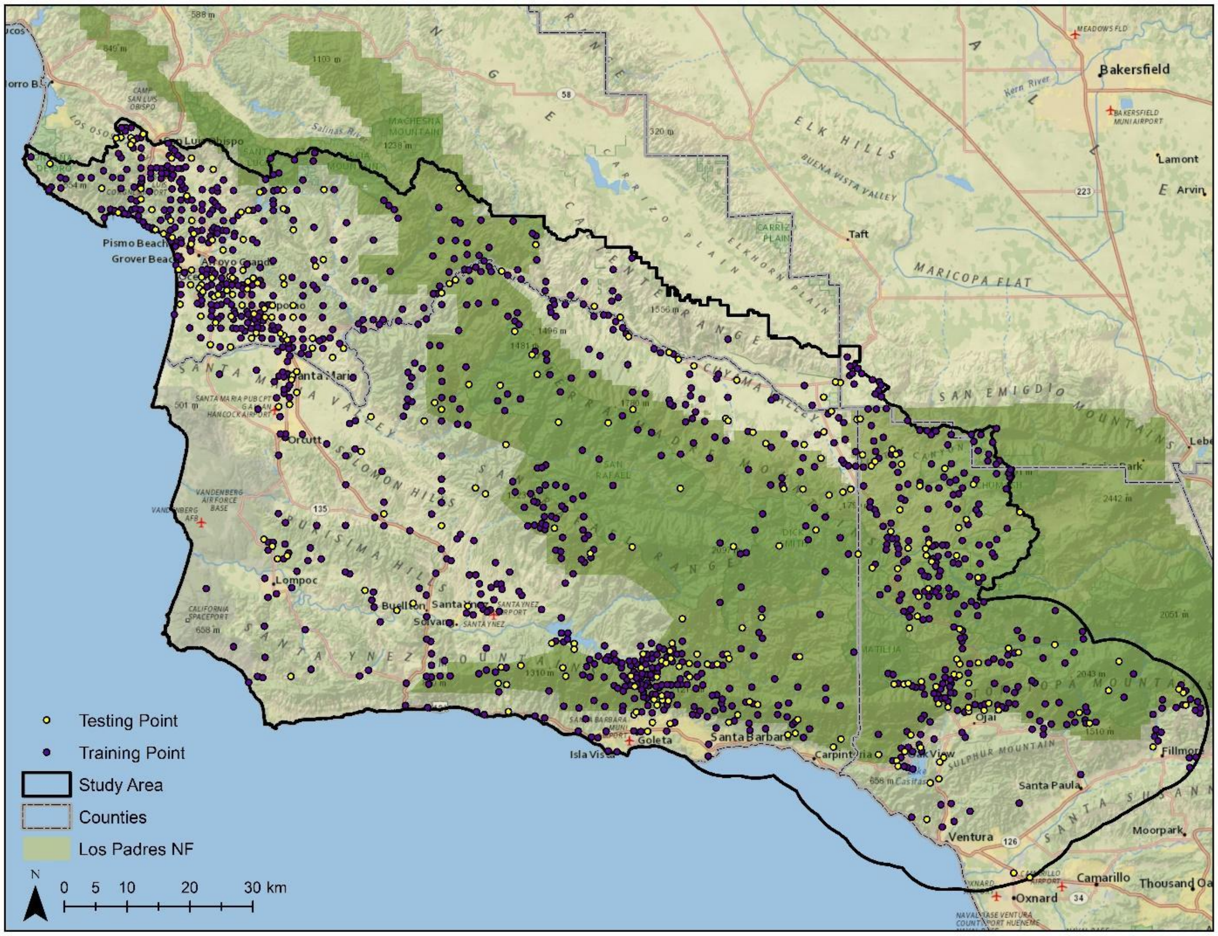

Figure 2. Fire ignition sample points from 1980-2019 used to train and test fire ignition model (also available in an interactive map).

For our large fire occurrence model, we used fire perimeter data for 201 large ($\geq$ 40-ha) fires from the State of California Fire and Resource Assessment Program (FRAP) fire history database[4], which covered our entire time period of interest. We generated a random sample of points within fire perimeters using the method developed by Davis et al. (2017): the number of random points generated within each fire perimeter was equal to the square root of the area within the perimeter divided by 40. As with the fire ignition point data, we also forced a minimum distance of 500 m between the random points. This process resulted in establishing 840 total sample points within large fire perimeters. We reserved 20% of those points for model evaluation, leaving a total of 669 points for model training (Figure 3).

[4] https://frap.fire.ca.gov/frap-projects/fire-perimeters/

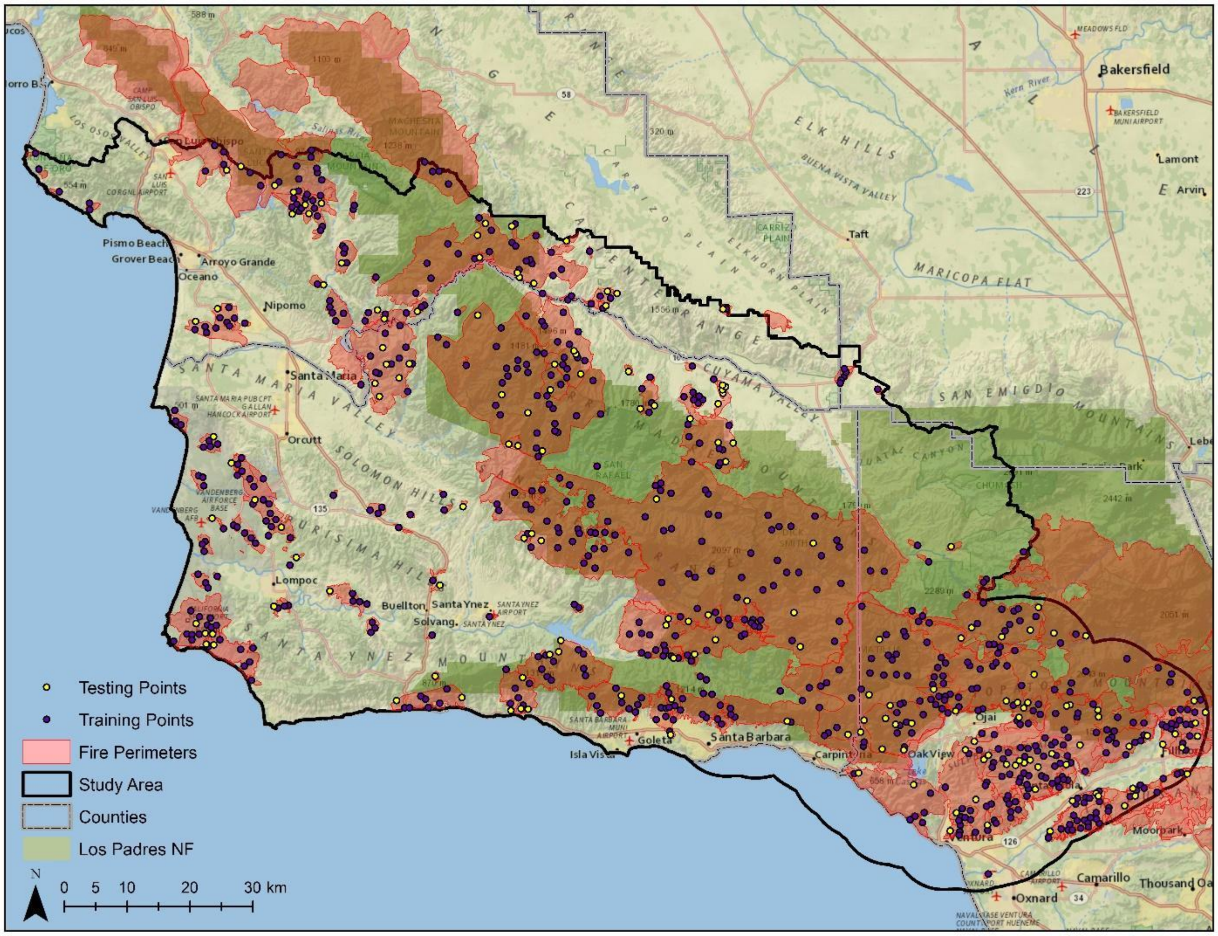

Figure 3. Sample points within large fires from 1980-2019 used to train and test large fire occurrence model (also available in an interactive map).

Environmental Predictor Data

We assembled datasets of 18 potential predictor variables at 270-m resolution characterizing ignition sources (because a fire must occur before it can develop into a large burn) and direct and indirect drivers of fire, such as climate, topography, land use, and vegetation (Table 1). This resolution was selected to match that of our downscaled climate data and as a compromise between that of the vegetation (800-m) and topographic predictors (30-m).

Several variables were tested to capture ignition susceptibility, both anthropogenic and natural (lightning). Anthropogenic factors also influence the likelihood of a fire growing and developing into a large fire, because fires closer to human population centers and roads are more likely to be detected and more accessible for rapid suppression and control. We therefore tested proximity to roads and proximity to development, which all have been found to be associated with human-caused fire ignitions and fire occurrence patterns (Parisien et al. 2012, Syphard and Keeley, 2015, Mann et al. 2016, Syphard et al. 2018, Syphard et al. 2019).

Table 1. Potential predictor variables considered for inclusion in fire ignition and large fire occurrence models.

Type	**Predictor**	**Time Period**	**Source**
Climate	Seasonality	1980-2010	CA BCM
Climate	Minimum Temperature	1980-2010	CA BCM
Climate	Mean Annual Precipitation	1980-2010	CA BCM
Climate	Mean Summer Precipitation	1980-2010	CA BCM
Climate	Climatic Water Deficit	1980-2010	CA BCM
Climate	Wind Speed, Average of 10 strongest Santa Ana Days	2004-2013	David Pierce, Scripps
Land Use	Distance to Roads (All)	2015	TIGER Roads
Land Use	Distance to Primary/Secondary Roads	2015	TIGER Roads
Land Use	Distance to Development	2016	NLCD Land Cover
Topography	Slope		LANDFIRE
Topography	Solar Insolation Index (2 – (sin((slope/90)180))*(cos(22 – aspect) + 1)), Gustafson et al. 2003		CBI/LANDFIRE
Topography	Southwestness (transformed slope aspect (cos(aspect-255)), Franklin 2003		CBI/LANDFIRE
Topography	Topographic Heterogeneity (standard deviation elevation calculated for center cell and three cell (90m) radius immediately surrounding)		NatureServe
Topography	Topographic Wetness Index (function of slope and upstream catchment area, calculated with SAGA GIS module)		CBI/LANDFIRE
Topography	Topographic Position		CBI/LANDFIRE
Vegetation (simulated)	Dead Wood Carbon	1980-2010	CBI/MC2
Vegetation (simulated)	Forest Carbon	1980-2010	CBI/MC2
Vegetation (simulated)	Standing Dead Grass Carbon	1980-2010	CBI/MC2

While spatial data for lightning strikes are available, they are too coarse in resolution to be useful in this application. Lightning-ignited fires are correlated with terrain complexity (McRae 1992, Vazquez and Moreno 1998, Kilinc and Beringer 2007) and fuel moisture (Podur et al. 2003; Wotton and Martell 2005), so we used terrain variables, such as topographic heterogeneity and slope, and fuel moisture variables, such as solar insolation index and topographic wetness index (a proxy for soil moisture) as potential lightning strike predictors.

Climate and weather are regarded as controlling factors of fire occurrence, size, and severity (Westerling et al. 2006, Littell et al. 2009, Dennison et al. 2014, Harvey et al. 2016). Such factors influence whether an ignition may develop into a large fire via effects on fuel moisture, structure, and abundance, as well as their real-time effects on fire behavior (e.g., due to wind). We therefore tested several temperature and precipitation variables, climatic water deficit (considered a proxy for fuel condition and moisture content), and wind speed for their influences on fire size (Table 1).

Following Parisien et al. (2012), Davis et al. (2017), Tracy et al. (2018), and Syphard et al. (2018 and 2019), we used long-term climate normals as references of relative conditions likely at each location. Climate normals represent the typical state based on averaged conditions from an area over decades of time (Davis et al. 2017). The use of long-term climate normals thus allows for projecting these models forward under different climate Coupled Model Intercomparison Project phase 5 (CMIP5) models, because downscaled projections are available as 30-year averages (CA-BCM 2014, http://climate.calcommons.org/dataset/2014-CA-BCM). Although finer-scale, real-time weather conditions during a fire would better predict actual fire effects, such data are difficult to assemble, and the scope of this project was to predict broad, general patterns to inform management decisions (e.g., forest restoration treatments), not to predict behavior of individual fires. We used the most recent 30-year time period (1980-2010) for which climate data are available as our baseline, and the immediate near term future (2020-2050) for projections. While climate projections for several CMIP-5 General Circulation Models are available from CA-BCM 2014, we were limited to those for which we also had outputs from the dynamic vegetation model. The two available, CNRM-CM5 (“cool/wet” conditions) and MIROC5 (“hot/dry” conditions), are GCMs recommended as priorities for research in California due to their range of relevant possible futures here (Kravitz 2017). We used the RCP 8.5 “business as usual” emissions scenario for both. We also tested a separate wind dataset, the average wind speed during the 10 strongest Santa Ana days, which was available for 2004-2013 only.

Vegetation is the fuel required for a wildfire to ignite and spread. Incorporating vegetation structure into a long-term fire model is difficult due to its highly dynamic nature relative to available vegetation data sets. We used in-house available simulated vegetation predictors derived from MC2 (Bachelet et al. 2015), a dynamic global vegetation model which simulates potential vegetation, carbon fluxes and pools, and wildfire, in place of static vegetation maps. MC2 was run at 800-m resolution under the fire suppression scenario (for more MC2 details, please see Syphard et al. 2018). We tested three MC2 simulated vegetation outputs as predictors: dead wood carbon, forest carbon, and standing dead grass carbon (Table 1).

Terrain is known to have a direct influence on fire behavior and to indirectly influence fuel flammability (Syphard et al. 2019). We therefore tested several terrain variables relating to topographic complexity, aspect, and exposure, including slope, solar insolation index, southwestness index, topographic wetness index (a proxy for soil moisture), and topographic heterogeneity (Table 1).

Modeling Process

Our modeling process consisted of 3 main steps: (1) variable selection (testing predictors independently and evaluating predictor collinearity), (2) multivariate model creation and variable pruning to create a parsimonious predictive model, and (3) model tuning to control for overfitting. Our models were run in MaxEnt using the default parameters, including model clamping, with the following exceptions: linear, quadratic, and product feature types only, and 10-fold cross-validated replication. Linear, quadratic, and product feature types are preferred to ensure smoother response curves (Santos et al. 2017) and because responses to ecological gradients are frequently nonlinear and interactions among predictors are common. Clamping restricts MaxEnt model extrapolations according to the limits of predictor variables used to train the model and is important when models are projected onto future conditions or new geographic areas.

Before using all candidate predictors in a full multivariate model, we conducted a correlation analysis on the predictors using ENMTools (version 1.4.4, Warren et al. 2010). To create more parsimonious and interpretable results (Merow et al. 2013), we excluded correlated variables ($|r| > 0.7$) by selecting the one with the highest univariate 10-fold cross-validated mean AUC (Area Under the Receiver Operating Characteristic (ROC) curve, a threshold-independent assessment of model discriminatory ability; Fielding and Bell 1997). Remaining predictors were carried forward to a full model.

We pruned the resulting full (multivariate) models in an iterative, stepwise process to increase model parsimony by removing the variable contributing the least information to model fit (highest mean training gain without the variable) to decrease model complexity and increase performance (Warren et al. 2014, Yiwen et al. 2016). The model was run again with the remaining predictors. This was repeated until only one variable remained. From the resulting model set, we selected the model with the fewest predictors having a mean training gain not significantly different from the full model. Significance was defined as lack of overlap of 95% confidence intervals for training gain means (calculated in R version 3.6.2; R Core Team 2013). While selected models may include predictors that seemingly have low importance, dropping these predictors results in a statistically significant decrease in model performance.

To prevent model overfitting and reduce complexity, we next tuned our selected model by varying MaxEnt's regularization multiplier parameter to constrain model complexity (Anderson and Gonzalez 2011, Merow et al. 2013, Radosavljevic and Anderson 2014*,* Warren et al. 2014). We varied the parameter from 0 to 5 in increments of 0.5 (default = 1), and used the ENMTools 'Model Selection' function to calculate AICc (Akaike information criterion corrected for small sample sizes) for each *(*Warren and Seifert 2011). For this analysis, MaxEnt was run with the variables from the selected pruned model, but using the 'raw' output and no replicates (required for model selection with ENMTools). We selected as the best model the one with the lowest AICc. AICc provides a quantitative measure balancing model complexity and goodness-of-fit without requiring a large independent evaluation dataset (Galante et al. 2018). The model with the lowest AICc is regarded as the best model tested, but all models with AICc values within 2 AICc units (dAICc) are considered to be supported and may be averaged using AICc weights. Rather than averaging models that vary only in terms of their regularization parameter if dAICc < 2, we instead opted for parsimony by simply selecting the regularization parameter with the minimum AICc.

We then ran MaxEnt with the logistic output option and 10-fold cross validation with the selected regularization parameters to get final output grids using our multivariate tuned models.

Model Evaluation

We evaluated the performance of our baseline models using both threshold-dependent and threshold-independent methods with fire data points reserved for testing along with an equal number of random 'pseudo-absence' points. For threshold-dependent, we used the maximum training sum of sensitivity and specificity (MAXSS), a model-specific threshold shown to optimize discrimination between presence and absence (Liu et al. 2013).

We used the MAXSS thresholds provided by MaxEnt to reclassify our continuous model outputs into binary 'high risk' (≥MAXSS) and 'low risk' (< MAXSS) grids. These were intersected with the reserved test and pseudo-absence points to calculate model sensitivity (True Positive /(True Positive + False Negative)), specificity (True Negative /(False Positive + True Negative)), precision (True Positive/(True Positive + False Positive), and accuracy ((True Positive + True Negative) / (Positive + Negative)).

Mean 10% test omission rates and difference between testing and training AUC values were examined to evaluate potential model overfitting. We also report test AUC values.

Model Projections

We ran MaxEnt a final time, using the projected future climate and simulated vegetation predictors in place of the baseline versions. We calculated percent change from baseline for each model and GCM.

Results

These results represent outputs from statistical models based on available landscape-scale GIS variables that cannot account for real-time fire conditions. They describe broad geographic patterns in landscape fire risk across Santa Barbara County. All model outputs should be considered hypotheses to be refined with additional information.

Fire Ignition Model

The anthropogenic factors tested, distance to development and distance to roads, are the most important predictors in the fire ignition model. Minimum temperature and annual precipitation also have moderate importance (Table 2). Fire ignition risk is highest both close to and far from roads and development, and lowest at moderate distances.

Fire ignition risk varies greatly across Santa Barbara County region, but is concentrated on flat slopes and in lower elevation areas, such as Nipomo Valley in the northwest, Santa Ynez Valley in the central part of the county, Cuyama Valley in the north, and Ojai Valley in the southeastern part of the study region (Figure 4). There is also a large zone at higher risk on the coast, in the greater Santa Barbara area.

Table 2. Predictor importance determined by MaxEnt for fire ignition and large fire occurrence risk models. NA indicates the predictor was not included.

Predictor	**Fire Ignition**	**Large Fire Occurrence**
Distance to Development	32.8	5.2
Distance to Roads (All)	22.5	NA
Minimum Temperature	12.5	17.3
Mean Annual Precipitation	10.1	12.7
Dead Wood Carbon	8.1	6.6
Mean Summer Precipitation	7.5	NA
Wind Speed, Average of 10 strongest Santa Ana Days	2.6	18.9
Topographic Wetness Index	1.8	NA
Slope	0.9	NA
Climatic Water Deficit	0.9	NA
Topographic Position	0.2	6.5
Topographic Heterogeneity	NA	22.8
Distance to Primary/Secondary Roads	NA	8.2
Southwestness	NA	1.8

Under CNRM-CM5, projected fire ignition risk patterns are similar to the baseline but the high risk footprint expands out along edges (Figure 5). Percent change from baseline is highest along mountainous areas (San Rafael and Santa Ynez), southwest of Lompoc, and in the Nipomo valley. Large decreases in fire ignition risk are projected under CNRM-CM5 in north-central and northeastern portions of the region (Caliente Range, Sierra Madre; Figure 6). Across the entire landscape, there is an average increase in projected fire ignition risk of 7%.

Under MIROC5, there is a projected contraction in areas of high fire ignition risk over most of the region, most notably in the greater Santa Barbara region, Santa Maria Valley, and Cuyama Valley (Figure 5). The very limited areas with increased projected fire ignition risk under MIROC5 are concentrated in inland areas at higher elevations, around Matilija Wilderness, Pine Mountain, and Topatopa Mountains (Figure 6), following patterns in increased summer precipitation and dead wood carbon. Across the entire landscape, there is an average decrease in projected fire ignition risk of 18% across landscape. Syphard et al. (2018) also noted higher projected mid-century fire ignition probabilities under CNRM relative to MIROC in Butte and Plumas counties.

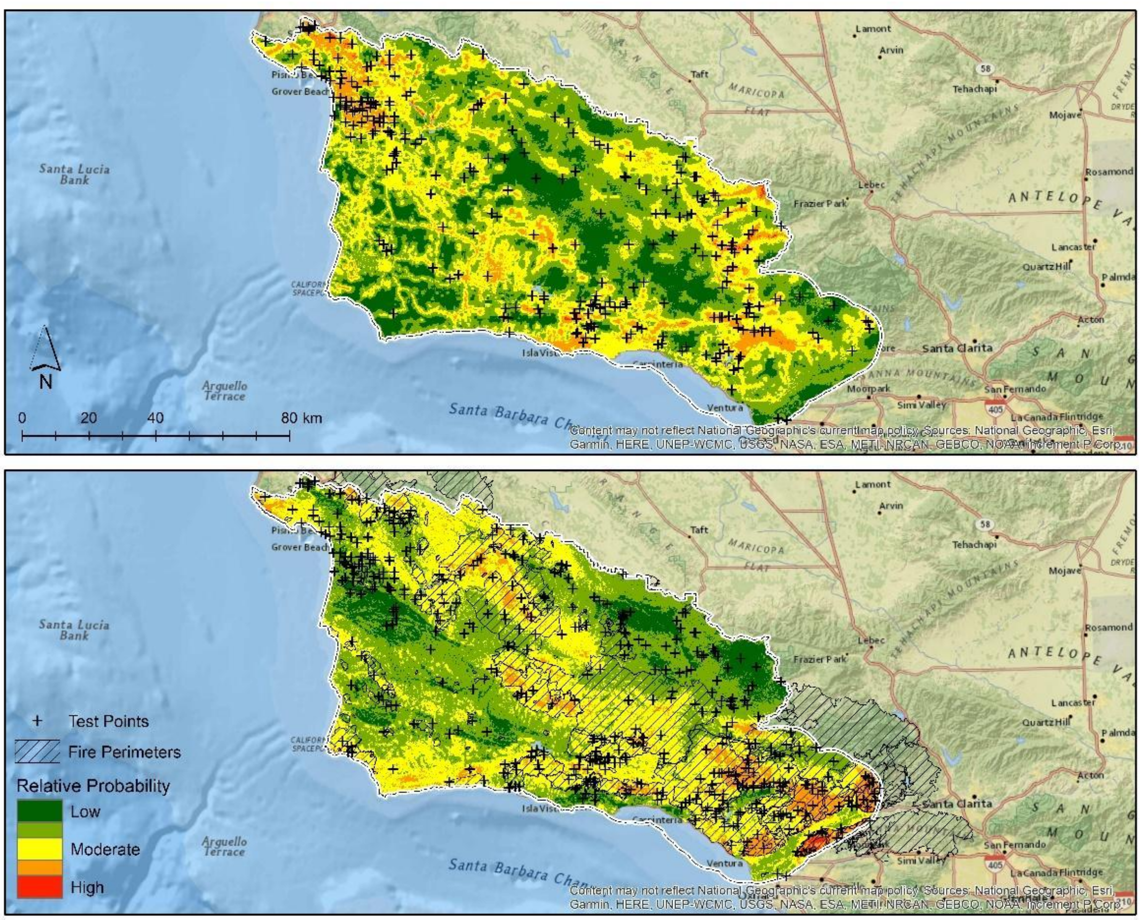

Figure 4. Modeled baseline fire ignition (top) and large fire occurrence (bottom) risk (also available in an [interactive map](#)).

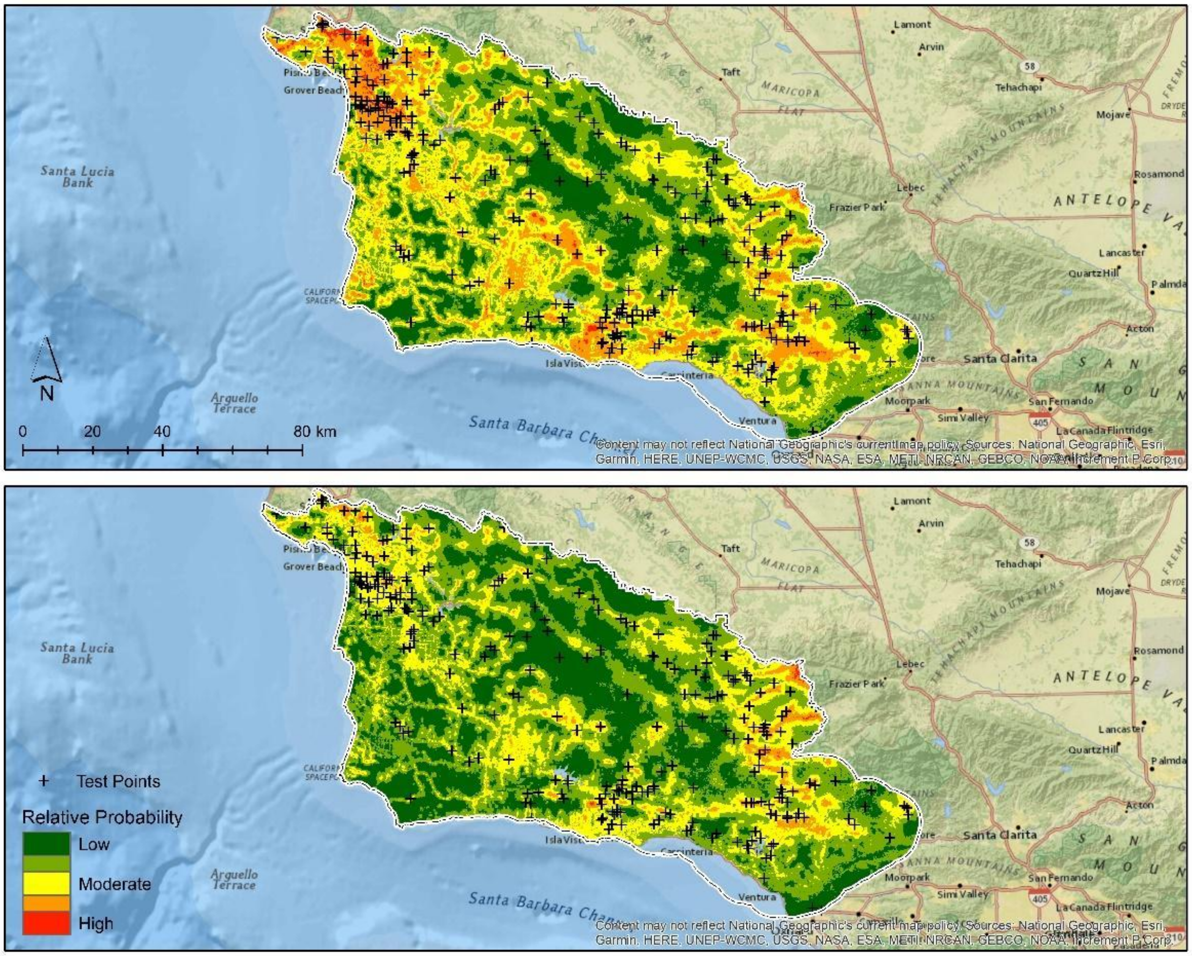

Figure 5. Projected fire ignition risk using CNRM-CM5 (top) and MIROC5 (bottom; also available in an [interactive map](#)).

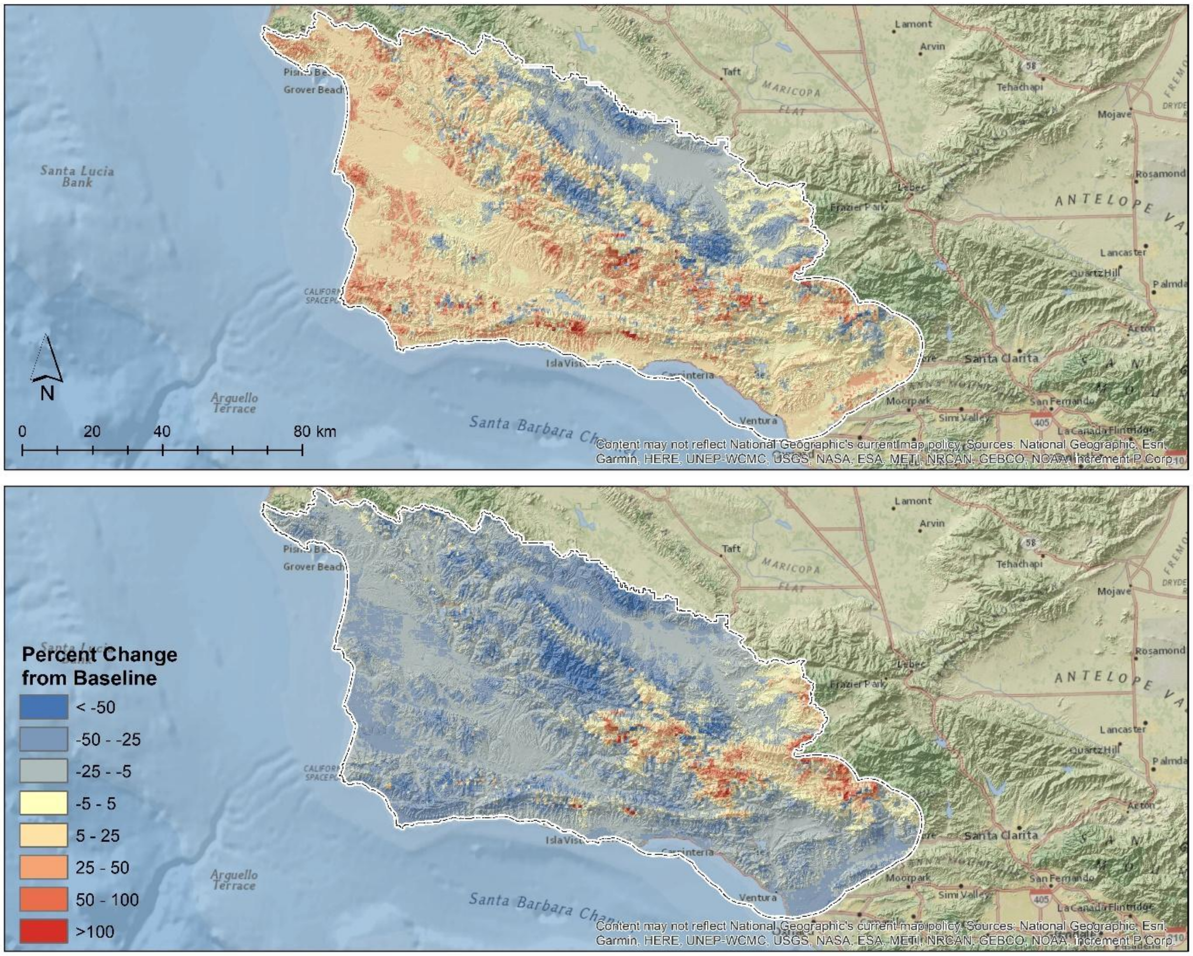

Figure 6. Projected percent change in fire ignition risk from baseline using CNRM-CM5 (top) and MIROC5 (bottom; also available in an interactive map).

Large Fire Occurrence Model

Climate and topographic predictors most strongly influenced the large fire occurrence model. Topographic heterogeneity, wind speed, minimum temperature, and annual precipitation were the most important variables (Table 2). Increased risk of large fires is associated with higher minimum temperature, higher annual precipitation, greater topographic complexity, and higher wind speeds.

Areas at greater risk for large fires in the region are at predominantly at higher elevations with steep slopes, along the Irish Hills in the west, Santa Ynez-Sulphur Mountains along the coast, Sierra Madre Mountains to the north, San Rafael Range in the central part of the region, and Topatopa Mountains to the east (Figure 4).

Under CNRM-CM5 and MIROC5, projected large fire occurrence risk patterns are similar to the baseline with the high risk footprint expanded along its margins (Figure 7). Minimum temperature and dead wood carbon, moderately important predictors in the large fire occurrence risk model, show similar patterns of increase relative to baseline under both GCMs. Percent change in projected large fire risk under CNRM-CM5 is highest in the northeastern part of the region around San Emigdio Mesa and San Guillermo Mountain, around the Topatopa Mountains in the east, and also along the Sierra Madre and San Rafael Mountains (Figure 8). There are little to no areas of projected decreasing large fire risk. Across the entire landscape, there is an average increase in projected large fire risk of 9% under CNRM-CM5. Highest projected increases in large fire risk are in small patches around San Emigdio Mesa and San Guillermo Mountain under MIROC5 (Figure 8), with an average increase of 8% across the landscape.

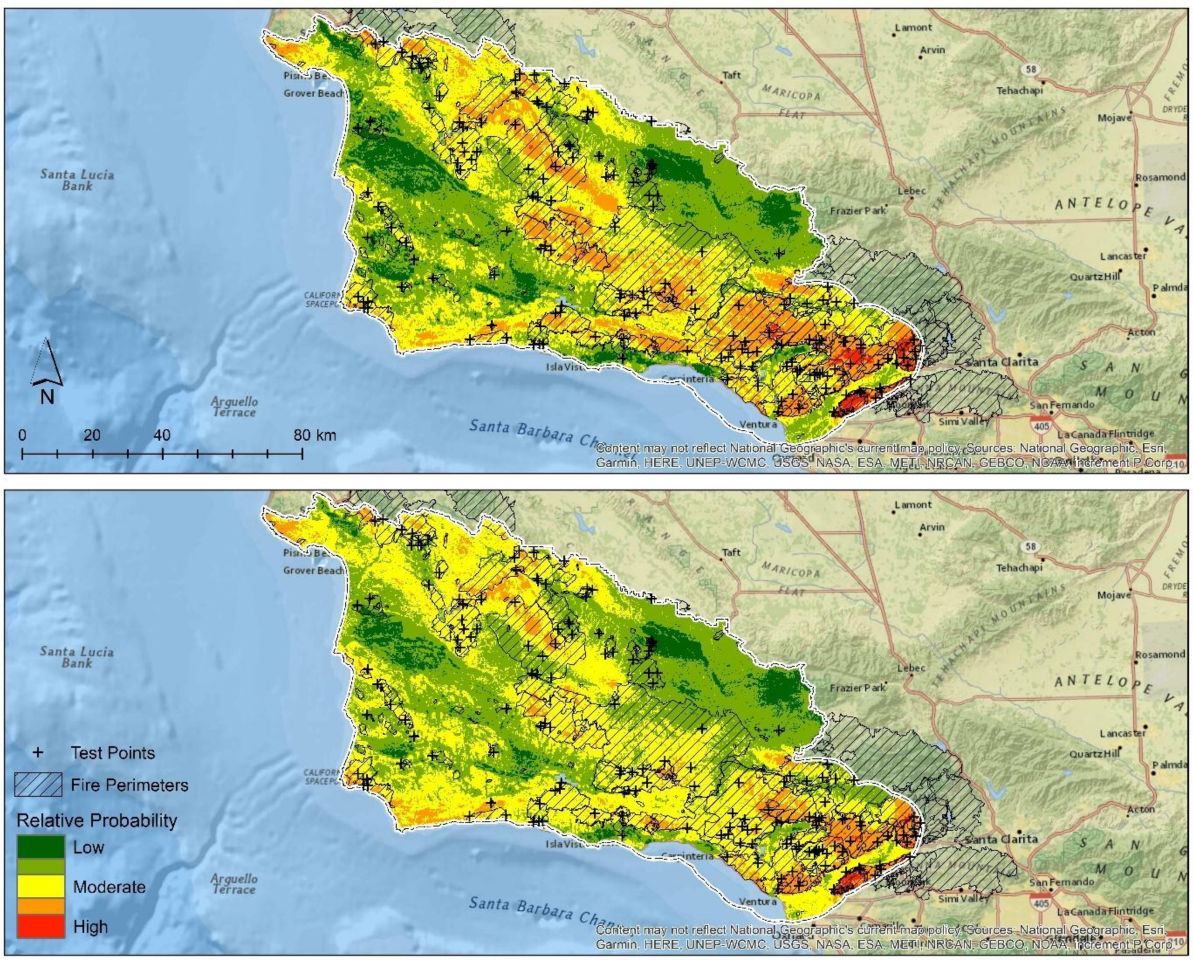

Figure 7. Projected large fire occurrence risk using CNRM-CM5 (top) and MIROC5 (bottom; also available in an [interactive map](#)).

Model Evaluation

The fire ignition and large fire occurrence risk models had similarly satisfactory performance, with average test AUC values (a measure of model discrimination) ranging from 0.72 for fire ignition to 0.67 for large fire occurrence (Table 3). Mean 10% test omission rates ranged from 0.10 to 0.11 and mean testing and training AUC values were very close for both models, suggesting neither suffered from overfitting.

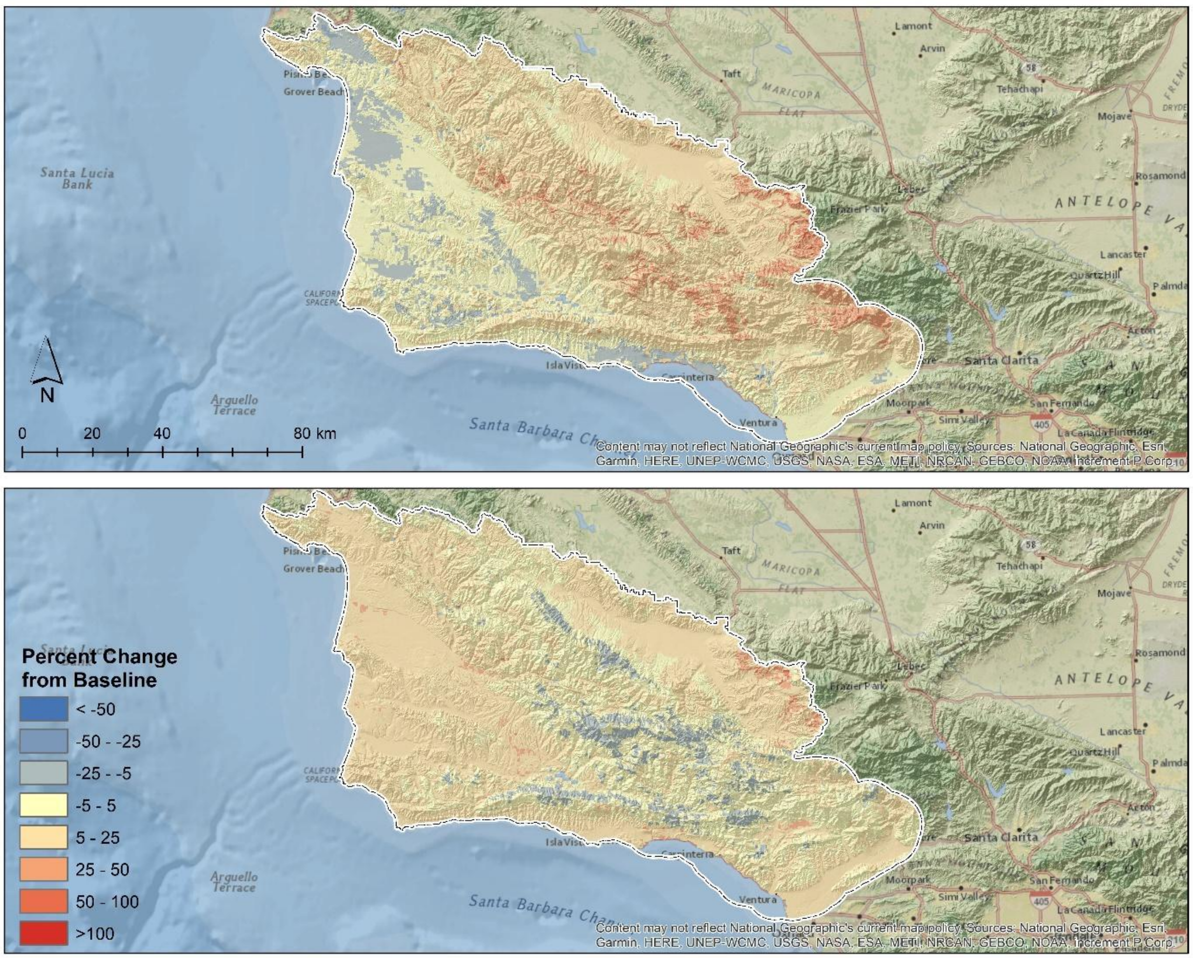

Figure 8. Projected percent change in large fire occurrence risk from baseline using CNRM-CM5 (top) and MIROC5 (bottom; also available in an interactive map).

Model sensitivity (proportion of fire model testing points correctly classified) ranged from 0.61 to 0.62, while specificity (proportion of fire model testing points correctly classified) ranged from 0.66 to 0.68 (Figure 9, Table 3). Overall accuracy was 0.64 for both models. AUC measured using reserved testing points was 0.70-0.71 (Figure 9, Table 3).

Both models have acceptable evaluation metrics, especially given that they do not account for real-time fire conditions and fire-fighting effects. We repeat that fire modeling is inherently uncertain given the stochastic nature of fire and how it is affected by factors not available for statistical analyses, and that these results must be interpreted with due caution.

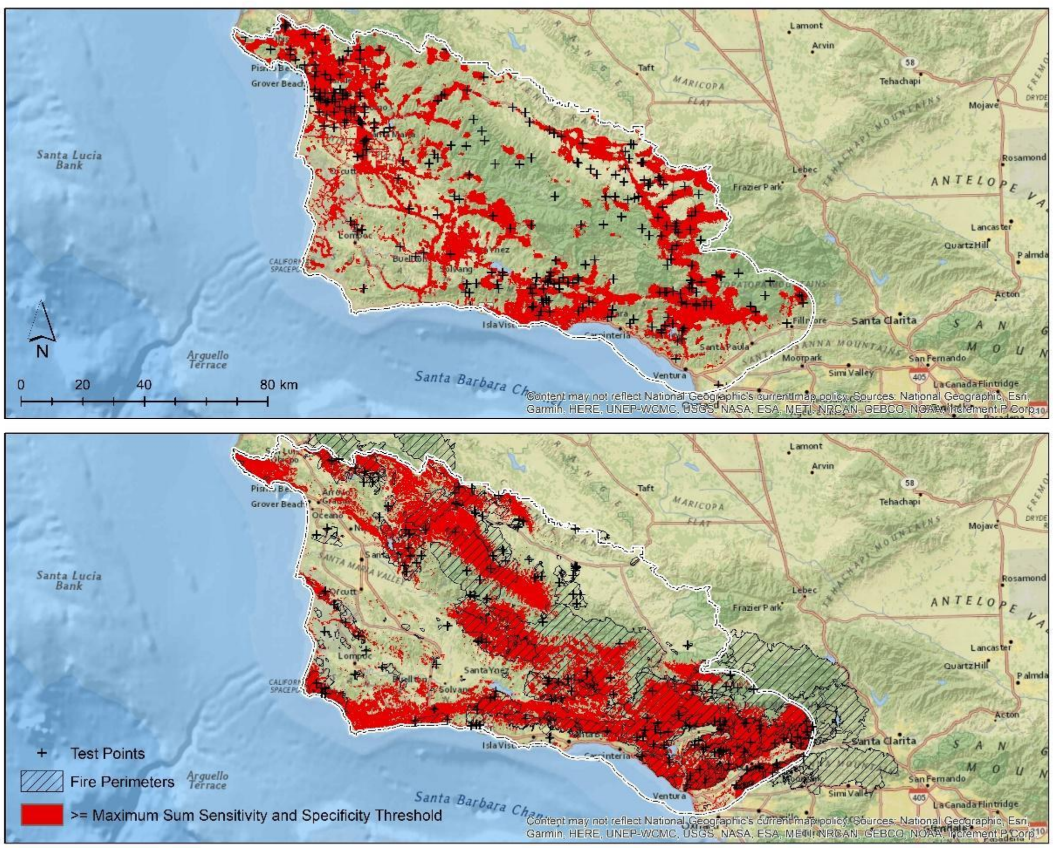

Figure 9. Modeled baseline fire ignition (top) and large fire occurrence (bottom) risk classified using maximum sum of sensitivity and specificity threshold for evaluation.

Table 3. Evaluation metrics for fire ignition and large fire occurrence risk models.

Metric	**Fire Ignition**	**Large Fire Occurrence**
Mean 10-fold Cross-Validated Test AUC	0.72	0.67
Mean 10-fold Cross-Validated Training AUC	0.73	0.69
Mean 10-fold Cross-Validated 10% Test Omission	0.11	0.10
Sensitivity	0.62	0.61
Specificity	0.66	0.68
Precision	0.66	0.67
Accuracy	0.64	0.64
Test AUC	0.71	0.70

Data Products

Results of this project are available as data layers that can be viewed and downloaded from Data Basin using the index below.

Map of all the below data layers:

1. Fire Risk Modeling Results, Santa Barbara County

Baseline Model Outputs:

1. Relative Probability of Fire Ignition, Santa Barbara County, Baseline
2. Relative Probability of Large Fires, Santa Barbara County, Baseline

Projections:

1. Relative Probability of Fire Ignition, CNRM-CM5, 2020-2050
2. Relative Probability of Fire Ignition, MIROC5, 2020-2050
3. Relative Probability of Large Fires, CNRM-CM5, 2020-2050
4. Relative Probability of Large Fires, MIROC5, 2020-2050

Percent Change Between Baseline and Projections:

1. Average Percent Change in Relative Probability of Fire Ignition
2. Percent Change in Relative Probability of Fire Ignition (CNRM-CM5)

3. Percent Change in Relative Probability of Fire Ignition (MIROC5)
4. Average Percent Change in Relative Probability of Large Fires
5. Percent Change in Relative Probability of Large Fires (CNRM-CM5)
6. Percent Change in Relative Probability of Large Fires (MIROC5)

Select Data Inputs:

1. Fire Ignition Sample Points, Santa Barbara County, 1980-2019
2. Large Fire Sample Points, Santa Barbara County, 1980-2019
3. Fire Perimeters, Santa Barbara County, 1980 - 2019

Literature Cited

Anderson, R.P. and I. Gonzalez, Jr. 2011. Species-specific tuning increases robustness to sampling bias in models of species distributions: an implementation with MaxEnt. Ecological Modelling 222: 2796-2811.

Bachelet, D., K., Ferschweiler, T.J. Sheehan, B.M. Sleeter, and Z. Shu. 2015. Projected carbon stocks in the conterminous US with land use and variable fire regimes. Global Change Biology 21(12): 4548-4560.

Bar-Massada, A., A.D. Syphard, S.I. Stewart, and V.C. Radeloff. 2012. Wildfire ignition-distribution modelling: a comparative study in the Huron–Manistee National Forest, Michigan, USA. International Journal of Wildland Fire 22: 174–183.

Boria, R.A., L.E. Olson, S.M. Goodman, and R.P. Anderson. 2014. Spatial filtering to reduce sampling bias can improve the performance of ecological niche models. Ecological Modelling 275: 73– 77.

Davis, R., Y. Zhiqiang, A. Yost, C. Belongie, and W. Cohen. 2017. The normal fire environment – Modeling environmental suitability for large forest wildfires using past, present, and future climate normals. Forest Ecology and Management 390: 173-186.

Dennison PE, S.C., Brewer, J.D. Arnold, and M.A. Moritz. 2014. Large wildfire trends in the western United States, 1984–2011. Geophysical Research Letters 41:2928–2933.

Fielding, A.H. and J.F. Bell. 1997. A review of methods for the assessment of prediction errors in conservation presence/absence models. Environmental Conservation 24: 38–49.

Franklin, J., 2003. Clustering versus regression trees for determining Ecological Land Units in the southern California Mountains and foothills. Forest Science 49: 354–368.

Galante, P.J., B. Alade, R. Muscarella, S.A. Jansa, S.M. Goodman, and R.P. Anderson. 2018. The challenge of modeling niches and distributions for data-poor species: a comprehensive approach to model complexity. Ecography 41: 726-736.

Gustafson, E.J., S.M. Lietz, and J.L. Wright. 2003. Predicting the spatial distribution of aspen growth potential in the upper Great Lakes region. Forest Science 49: 499-508.

Harvey, B.J., D.C. Donato, and M.G. Turner. 2016. Drivers and trends in landscape patterns of stand-replacing fire in forests of the US Northern Rocky Mountains (1984-2010). Landscape Ecology 31: 2367-2383.

Kilinc, M. and J. Beringer. 2007. The spatial and temporal distribution of lightning strikes and their relationship with vegetation type, elevation, and fire scars in the Northern Territory. Journal of Climate 20: 1161-1173.

Kravitz, R. 2017. Projected Climate Scenarios Selected to Represent a Range of Possible Futures in California. Sacramento CA. Available from http://docketpublic.energy.ca.gov/PublicDocuments/16-IEPR-04/TN215798_20170207T111409_Projected_Climate_Scenarios_Selected_to_Represent_a_Range_of_Po.pdf

Littell, J.S., D. McKenzie, D.L. Peterson, and A.L. Westerling. 2009. Climate and wildfire area burned in western U.S. ecoprovinces, 1916–2003. Ecological Applications 19:1003-1021.

Liu, C., M. White, and G. Newell. 2013. Selecting thresholds for the prediction of species occurrence with presence-only data. *Journal of Biogeography* 40(4):778-789.

Mann, M.L., E. Batllori, M.A. Moritz, E.K. Waller, P. Berck, A.L. Flint, L.E. Flint, and E. Dolfi. 2016. Incorporating anthropogenic influences into fire probability models: effects of human activity and climate change on fire activity in California. PLoS One 11(4): e0153589.

McRae, R.H.D. 1992. Prediction of areas prone to lightning ignition. International Journal of Wildland Fire 2:123-130.

Merow, C., M.J. Smith, and J.A. Silander, Jr. 2013. A practical guide to MaxEnt for modeling species’ distributions: what it does, and why inputs and settings matter. Ecography 36: 1058-1069.

Parisien, M.-A., S. Snetsinger, J.A. Greenberg, C.R. Nelson, T. Schoennagel, S.Z. Dobrowski, and M.A. Moritz. 2012. Spatial variability in wildfire probability across the western United States. International Journal of Wildland Fire 21: 313-327.

Parisien, M.-A., S. Snetsinger, J.A. Greenberg, C.R. Nelson, T. Schoennagel, S.Z. Dobrowski, and M.A. Moritz. 2016. The spatially varying influence of humans on fire probability in North America. Environmental Research Letters 11:75005.

Phillips, S. J., R. P. Anderson, and R. E. Schapire. 2006. Maximum entropy modeling of species geographic distributions. Ecological Modelling 190:231-259.

Podur, J., D.L. Martell, F. Csillag. 2003. Spatial patterns of lightning-caused forest fires in Ontario, 1976-1998. Ecological Modelling 164: 1-20.

Radosavljevic, A. and R.P. Anderson. 2014. Making better MaxEnt models of species distributions: complexity, overfitting and evaluation. Journal of Biogeography 41: 629–643.

Santos, M.J., A.B. Smith, J.H. Thorne, and C. Moritz. 2017. The relative influence of change in habitat and climate on elevation range limits in small mammals in Yosemite National Park, California, U.S.A. Climate Change Responses 4:7.

Syphard, A.D. and J.E. Keeley. 2015. Location, timing, and extent of wildfire varies by cause of ignition. International Journal of Wildland Fire 24: 37–47.

Syphard, A.D., T. Sheehan, H. Rustigian-Romsos, and K. Ferschweiler. 2018. Mapping future fire probability under climate change: Does vegetation matter? PloS one 13: e0201680.

Syphard, A.D., H. Rustigian-Romsos, M. Mann, E. conlisk, M.A. Moritz, and D. Ackerly. 2019. The relative influence of climate and housing development on current and projected future fire patterns and structure loss across three California landscapes. Global Environmental Change 56: 41-55.

Tracy, J.L., A. Trabucco, A.M. Lawing, J. T. Giermakowski, M. Tchakerian, G.M. Drus, and R.N. Coulson. 2018. Random subset feature selection for ecological niche models of wildfire activity in Western North America. Ecological Modelling 383:52–68.

Vazquez, A. and J.M. Moreno. 1998. Patterns of lightning-, and people-caused fires in peninsular Spain. International Journal of Wildland Fire 8: 103-115.

Veloz, S.D. 2009. Spatially autocorrelated sampling falsely inflates measures of accuracy for presence-only niche models. Journal of Biogeography 36: 2290–2299.

Warren, D.L., R.E. Glor, and M. Turelli. 2010. ENMTools: a toolbox for comparative studies of environmental niche models. Ecography 33: 607-611.

Warren, D.L., A.N. Wright, S.N. Seifert, and B.H. Shaffer. 2014. Incorporating model complexity and spatial sampling bias into ecological niche models of climate change risks faced by 90 California vertebrate species of concern. Diversity and Distributions 20: 334–343.

Westerling, A.L., H.G. Hidalgo, D.R. Cayan, and T.W. Swetnam. 2006. Warming and earlier spring increases western US forest wildfire activity. Science 313: 940–943.

Wotton, B.M. and D.L. Martell. 2005. A lightning fire occurrence model for Ontario. Canadian Journal of Forest Research 35: 1389-1401.

Yiwen, Z., B.W. Low, and D.C.J. Yeo. 2016. Novel methods to select environmental variables in MaxEnt: A case study using invasive crayfish, Ecological Modelling 341: 5-13.

Appendices

Appendix 1. Correlation matrix of predictors across study area.

	cwd	dist_allrds	dist_dev	dist_psrds	insol	ndvimax	ppt_ann	ppt_summ	slope	sw	tmean_co	tmin_min	topoheter	tpi_1km_	tpi_2500m	twi
wind_mag	-0.01	0.23	0.23	0.28	-0.19	-0.08	0.24	0.16	0.27	-0.01	0.35	-0.16	0.29	0.04	0.06	-0.19
cwd		-0.15	-0.01	-0.15	-0.01	-0.19	-0.46	-0.20	-0.07	-0.03	0.14	0.16	-0.13	0.02	0.01	-0.04
dist_allrds			0.48	0.54	-0.22	-0.11	0.41	0.20	0.41	-0.04	0.44	-0.38	0.43	0.07	0.10	-0.30
dist_dev				0.43	-0.22	-0.02	0.34	0.22	0.44	-0.08	0.55	-0.36	0.43	0.03	0.09	-0.21
dist_psrds					-0.24	-0.05	0.45	0.27	0.45	-0.03	0.45	-0.32	0.46	0.08	0.10	-0.36
insol						-0.05	-0.33	-0.15	-0.46	0.32	-0.24	0.09	-0.47	-0.24	-0.26	0.50
ndvimax							0.31	-0.10	0.11	-0.06	-0.31	0.31	0.14	0.10	0.12	-0.10
ppt_ann								0.21	0.55	-0.07	0.27	-0.14	0.61	0.14	0.18	-0.41
ppt_summer									0.24	-0.02	0.37	-0.49	0.25	0.10	0.15	-0.22
slope										-0.11	0.47	-0.21	0.90	0.20	0.29	-0.70
sw											-0.06	0.02	-0.11	-0.05	-0.05	0.14
tmean_cov												-0.69	0.48	0.12	0.15	-0.41
tmin_min													-0.20	-0.04	-0.04	0.20
topohetero														0.20	0.29	-0.66
tpi_1km_6cl															0.95	-0.47
tpi_2500m_6cl																-0.50

Appendix 2. Model response plots.

A. Fire ignition model

a. Univariate plots

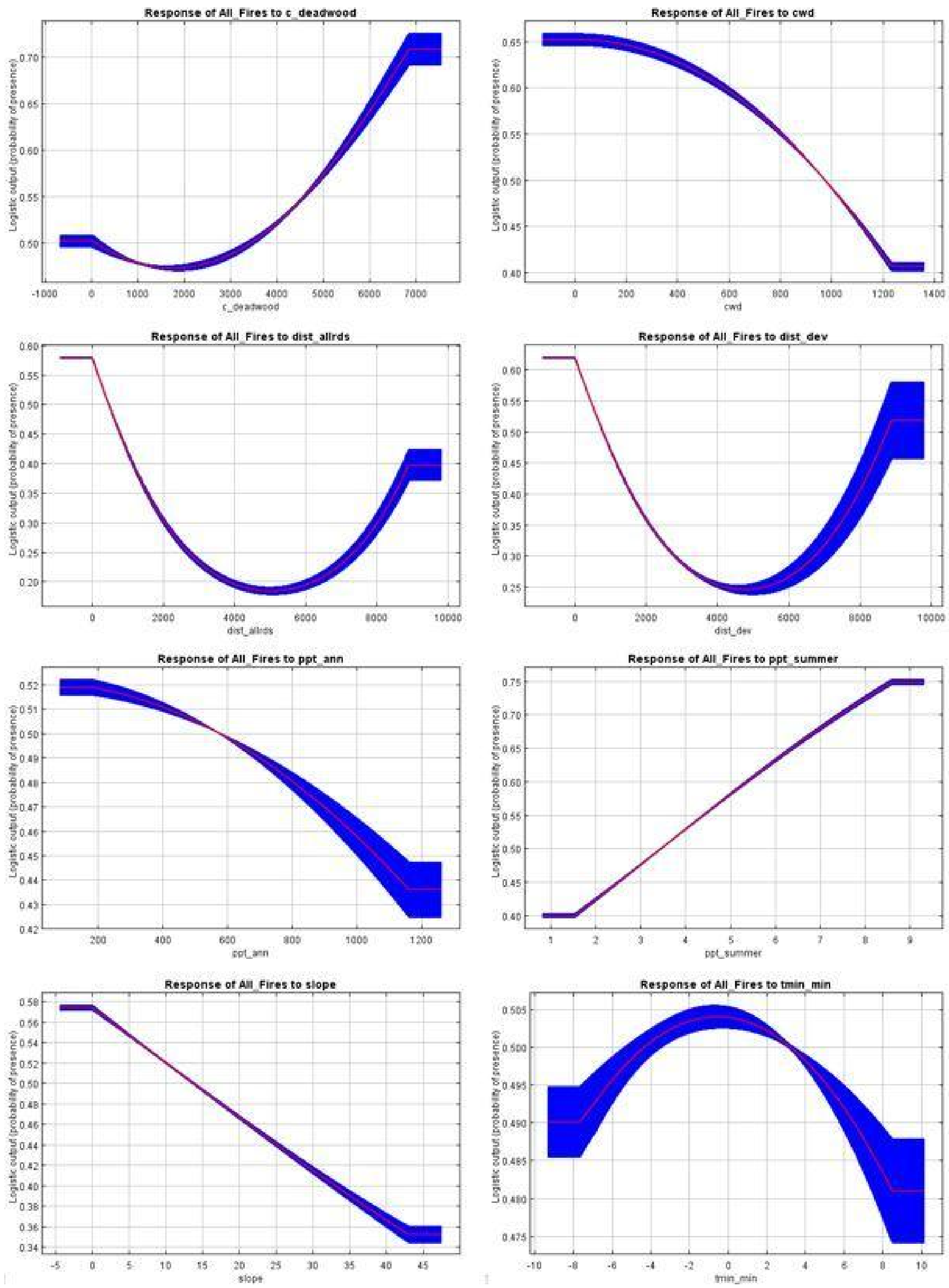

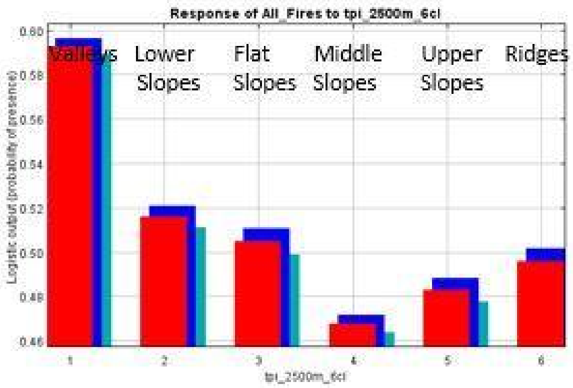
Response of All_Fires to tpi_2500m_6cl
Valleys
Lower Slopes
Flat Slopes
Middle Slopes
Upper Slopes
Ridges
Logistic output (probability of presence)
tpi_2500m_6cl

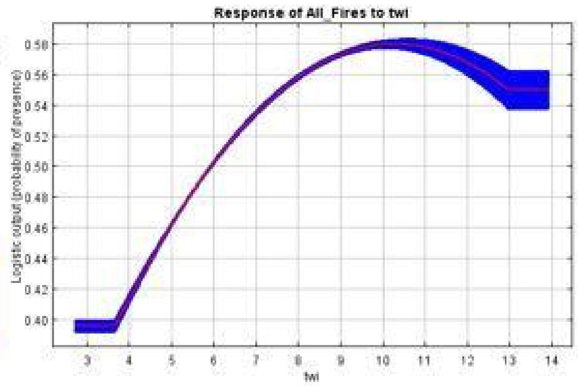
Response of All_Fires to twi
Logistic output (probability of presence)
twi

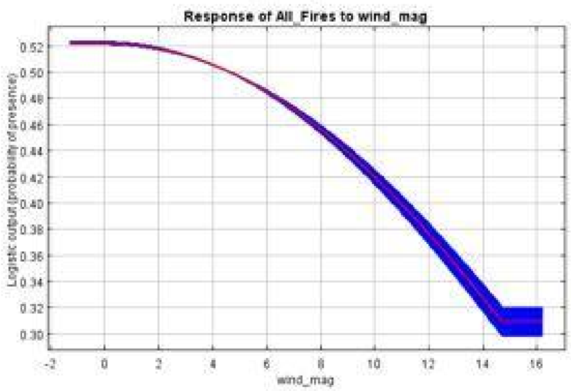
Response of All_Fires to wind_mag
Logistic output (probability of presence)
wind_mag

b. Marginal plots

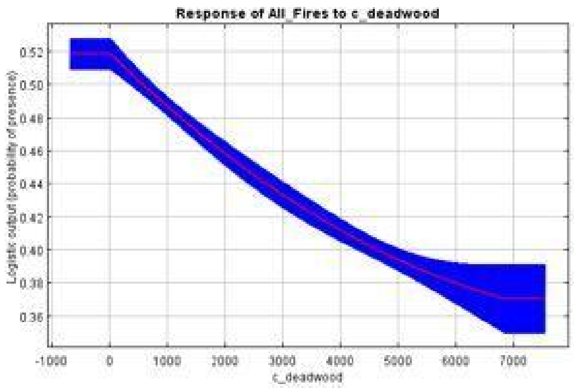

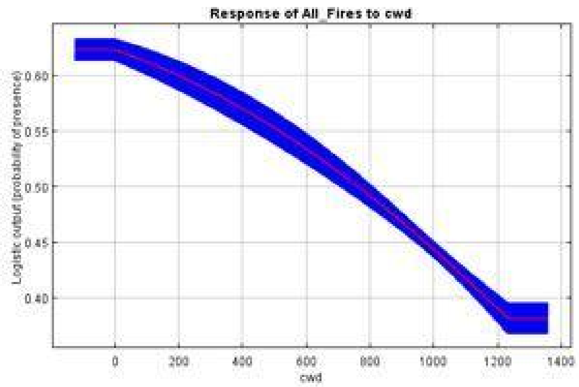

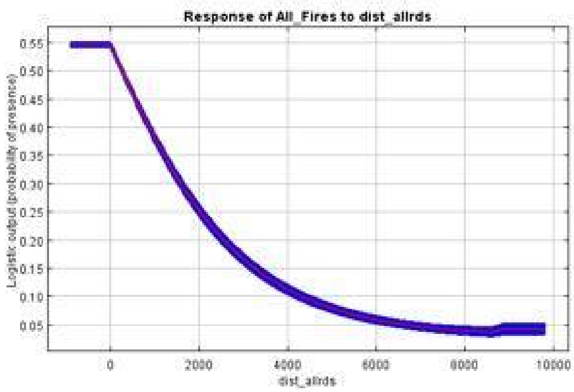

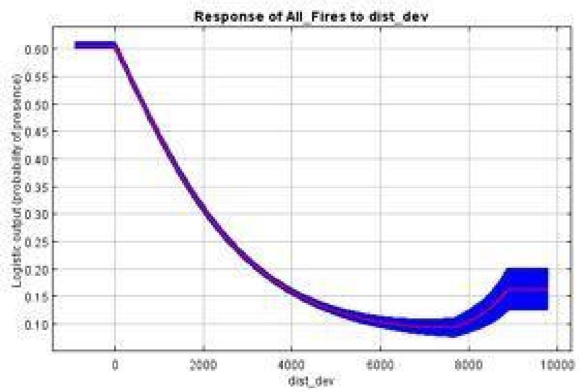

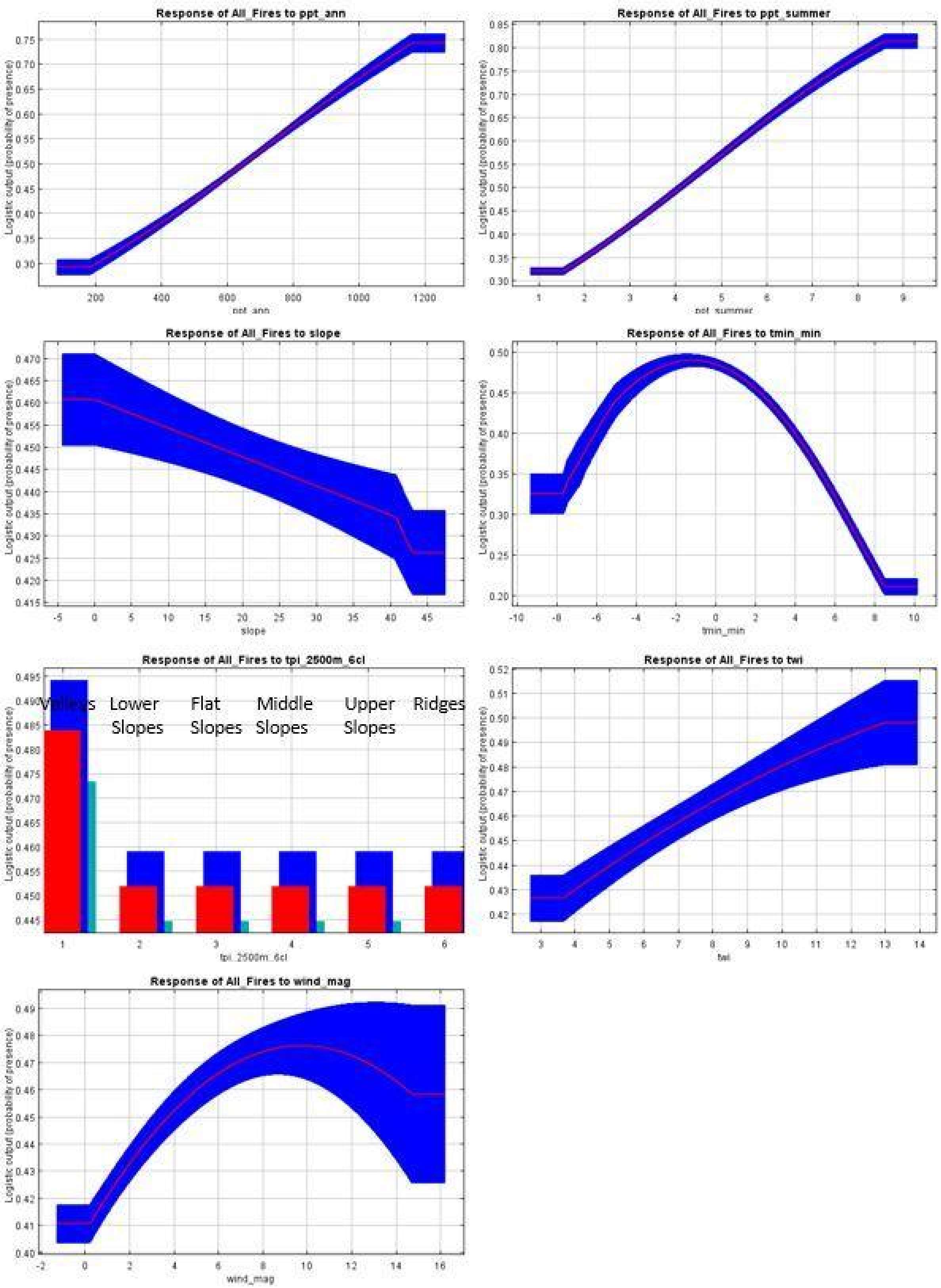
Response of All_Fires to ppt_ann
Logistic output (probability of presence)
ppt_ann
Response of All_Fires to ppt_summer
ppt_summer
Response of All_Fires to slope
slope
Response of All_Fires to tmin_min
tmin_min
Response of All_Fires to tpi_2500m_6cl
Valleys
Lower Slopes
Flat Slopes
Middle Slopes
Upper Slopes
Ridges
tpi_2500m_6cl
Response of All_Fires to twi
twi
Response of All_Fires to wind_mag
wind_mag

B. Large fire occurrence model

a. Univariate plots

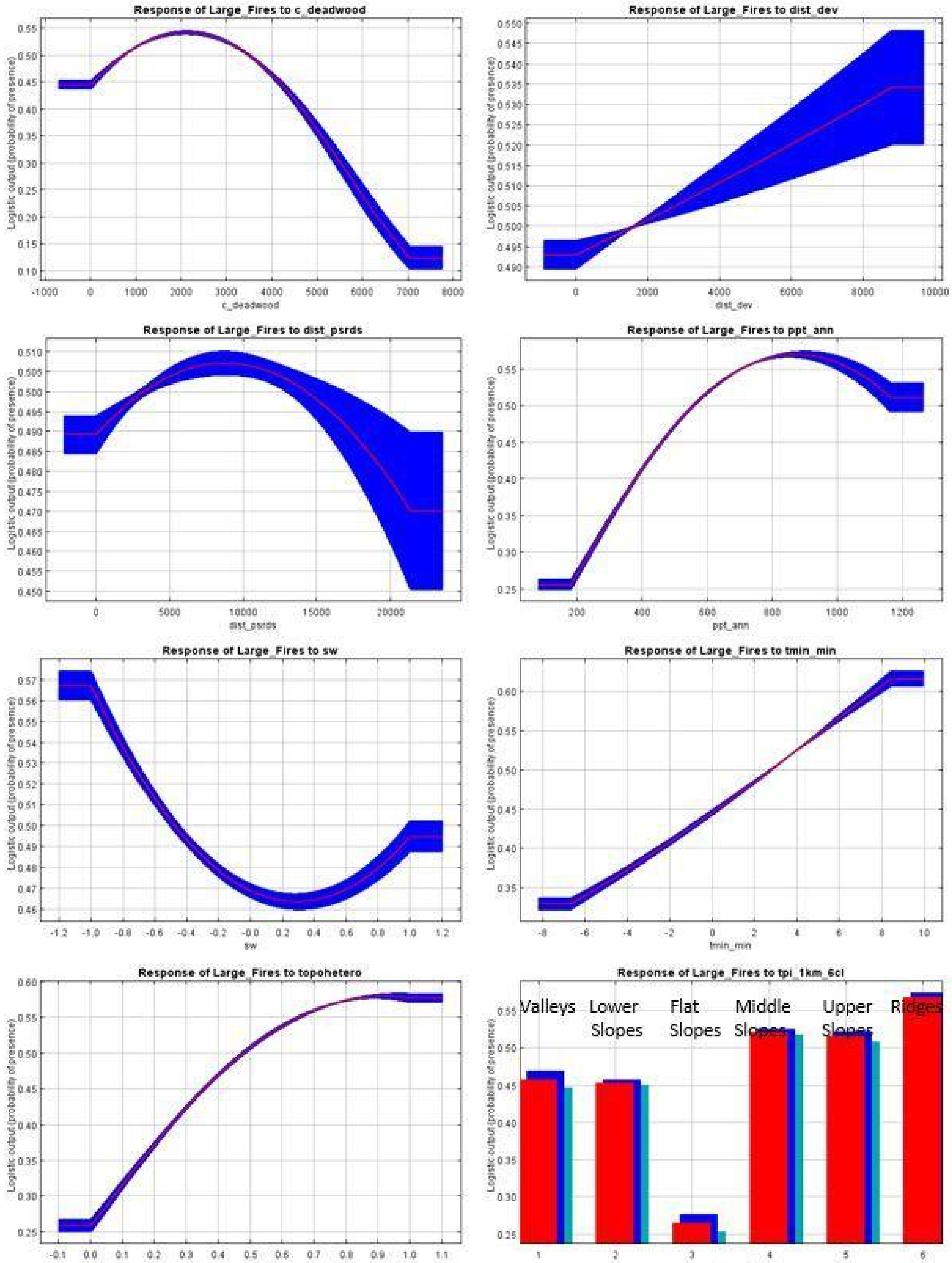

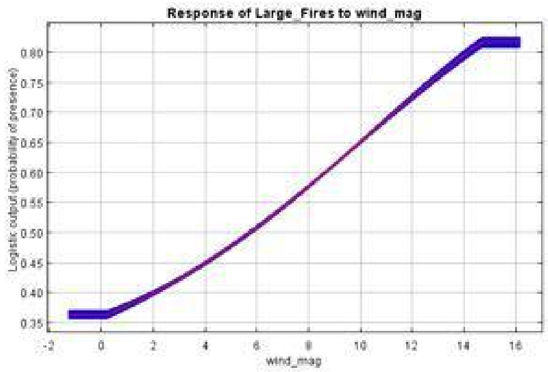
Response of Large_Fires to wind_mag
Logistic output (probability of presence)
0.80
0.75
0.70
0.65
0.60
0.55
0.50
0.45
0.40
0.35
-2
0
2
4
6
8
10
12
14
16
wind_mag

b. Marginal plots

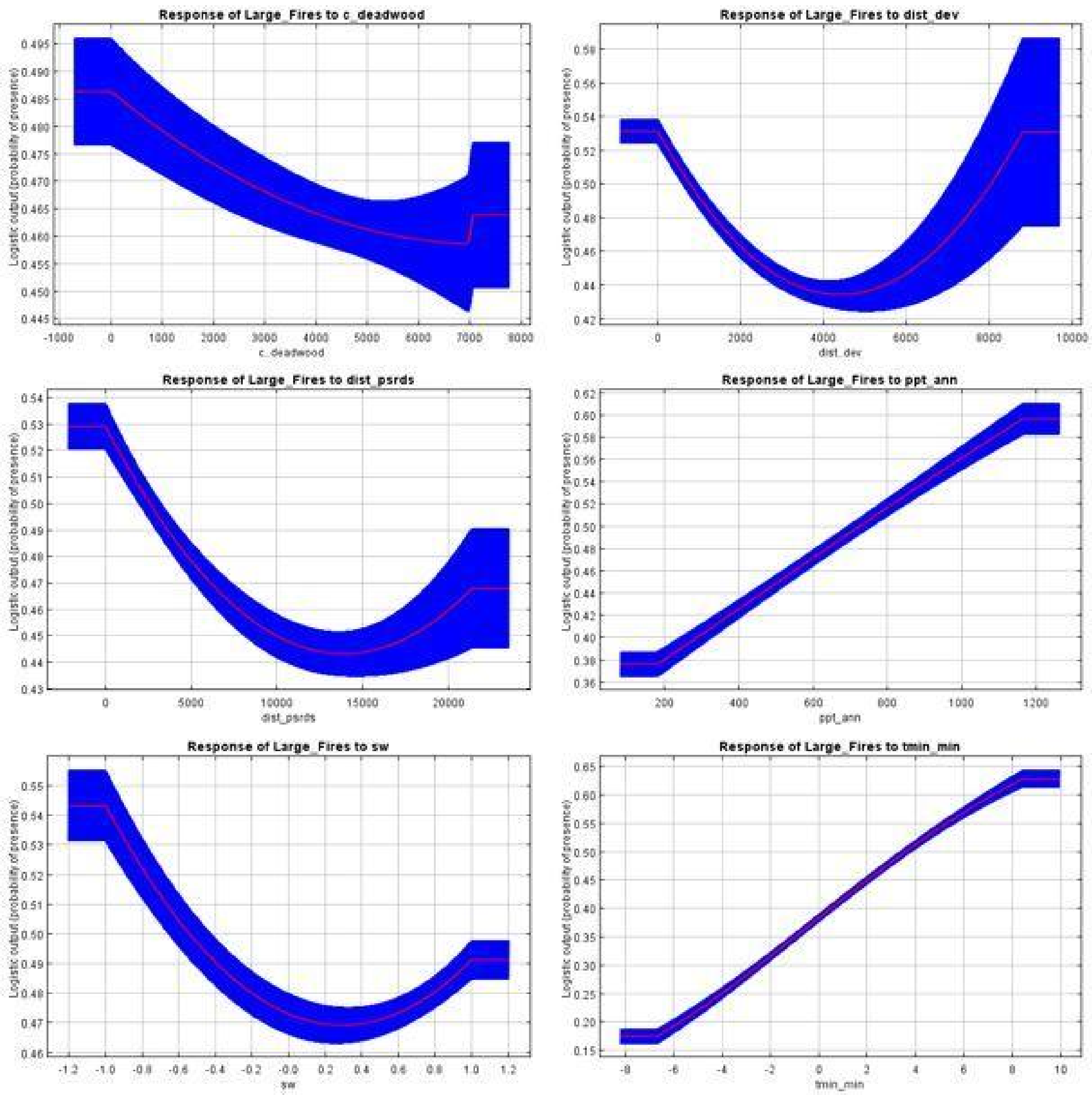

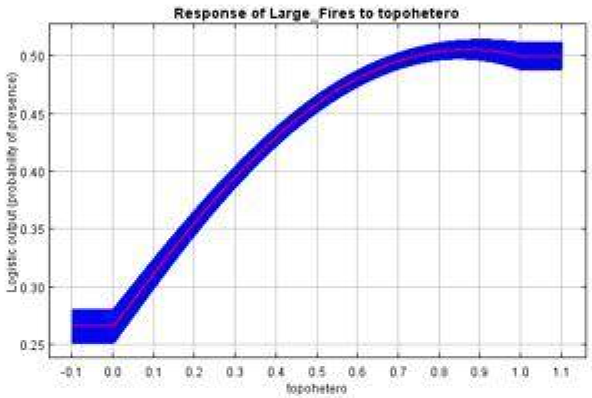
Response of Large_Fires to topohetero
Logistic output (probability of presence)
topohetero

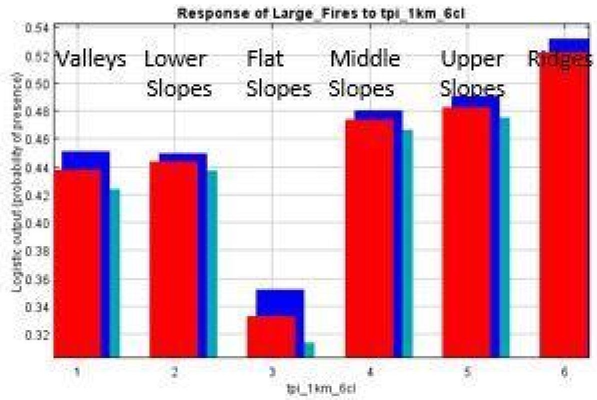
Response of Large_Fires to tpi_1km_6cl
Valleys
Lower Slopes
Flat Slopes
Middle Slopes
Upper Slopes
Ridges
Logistic output (probability of presence)
tpi_1km_6cl

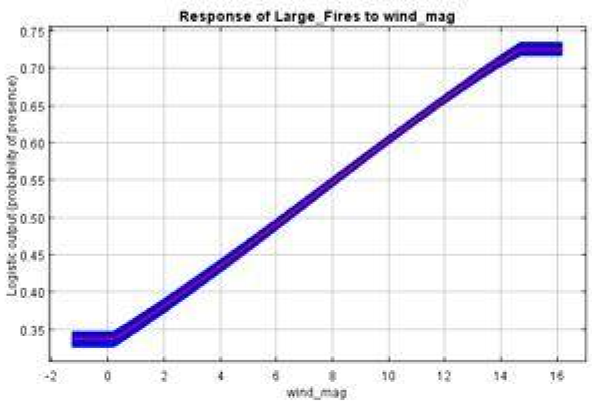
Response of Large_Fires to wind_mag
Logistic output (probability of presence)
wind_mag